24th COBEM - 2017

24th ABCM International Congress of Mechanical Engineering
December 3-8, 2017, Curitiba, PR, Brazil

COBEM-2017-0135
3D PRINTED PLA AND PLA REINFORCED WITH SHORT CARBON FIBERS: AN EXPERIMENTAL CHARACTERIZATION

Rafael Thiago Luiz Ferreira
Igor Cardoso Amatte
Thiago Assis Dutra
ITA - Aeronautics Institute of Technology
GPMA - Research Group on Additive Manufacturing
DCTA ITA IEM, 12228-900, São José dos Campos, São Paulo, Brazil
rthiago@ita.br, igamatte@gmail.com, thiagoassis.dutra@gmail.com

Daniel Bürger
FAB - Brazilian Air Force
IAE - Institute of Aeronautics and Space
AMR - Materials Division
DCTA IAE AMR, 12228-900, São José dos Campos, São Paulo, Brazil
burgerdb@iae.cta.br

Abstract. *In this paper, mechanical properties of the 3D printing materials PLA and PLA+CF are determined by experiments. The PLA (polylactic acid) is a base polymer and the PLA+CF is a composite formed by PLA reinforced with chopped carbon fibers in a weight fraction of 15%. The specimens tested are printed using the FDM (fused feposition modelling) process. Regarding that the plane of printing is the 1-2, the goal is to obtain for both PLA and PLA+CF the E_1 and E_2 tensile elastic moduli, the ν_{12} and ν_{21} Poisson ratios and the G_{12} shear elastic modulus, together with strength related properties (tensile S_1^*, S_2^* and shear S_{12}^*). The results obtained are used to evaluate the carbon fibers reinforcement in PLA. SEM (scanning electron microscopy) are also used to explain differences found in the PLA and PLA+CF properties. It is concluded that the short carbon fibers consistently raised the PLA+CF stiffness in the direction of printing, but are not able to improve its strengths.*

Keywords: *3D printing, carbon fiber composites, experimental material properties*

1. INTRODUCTION

3D printing is rapidly evolving and gaining popularity. One of the main reasons for this growth is the open source design of several 3D printing equipments, which motivates the final users to also participate in such equipments development. Moreover, 3D printing permits to a person to produce goods in home, under demand and with relatively low costs. The printed parts usually do not require further machining or tooling to be ready to use.

A key process in 3D printing is the FDM (fused feposition modelling) (Upcraft and Fletcher, 2003; Chua and Leong, 2017), where a thermoplastic polymer is fused and selectively deposited in a printing bed, forming the desired component. One of the fronts where development efforts are nowadays concentrated is the mechanical quality of the materials employed in 3D printing by FDM. To obtain functional components, reinforcements such as carbon, glass and kevlar fibers are added to base polymers that are used in FDM, in order to enhance stiffness and strength of the printed parts (Ning *et al.*, 2015; Wang *et al.*, 2017).

The objective of this work is the experimental mechanical characterization of two materials employed in FDM: a base polymer and the same polymer with reinforcements. The base polymer is a PLA (polylactic acid) and the reinforced material is a PLA with adittion of chopped short carbon fibers (PLA-CF), of length about $60\mu m$ and in a weight volume of 15%. Considering that 1-2 is the plane of 3D printing, the objetive is to obtain the E_1 and E_2 tensile elastic moduli, the ν_{12} and ν_{21} Poisson ratios and the G_{12} shear elastic modulus, for both materials. Strength related properties are also obtained, the S_1^* and S_2^* tensile strengths and the S_{12}^* shear strength. The quantities acquired are compared in order to assess the influence of the carbon fiber reinforcements in the PLA base material.

For all the experiments, the main assumption followed is that a 3D printed specimen behaves like a laminated material with oriented layers (Reddy, 1997). Figure 1 illustrates global and local material directions considered in this study. The orientations used in specimens are detailed in the next section.

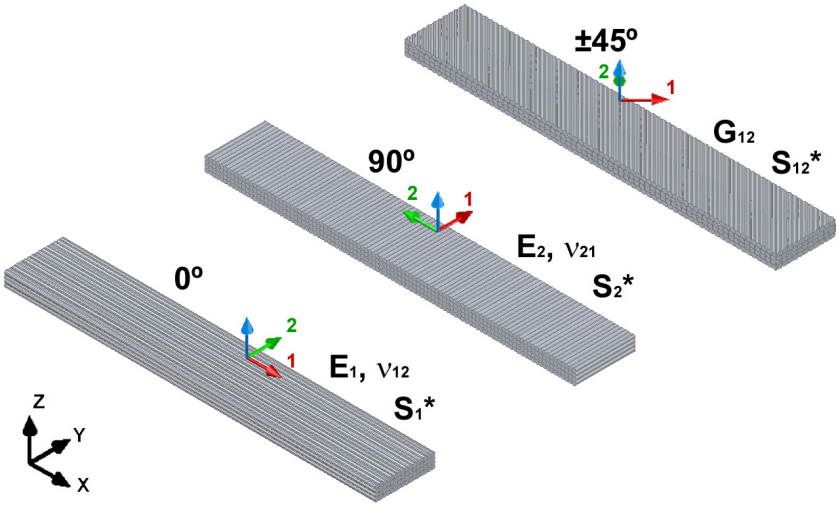

Figure 1: The local material directions are 1, the direction of printing, and 2, perpendicular to 1. The global coordinates are x,y,z. Illustration of printing orientations ($0°$, $90°$ and $\pm 45°$).

2. METHODOLOGY

Albeit there is a standard on making technical reports about 3D printed test specimens (ASTM F2971-13), there are not, up to now, specific standards for the mechanical testing of 3D printed materials, based on the authors' best knowledge. Therefore, to fullfill the objective of this work, test standards for polymers and laminated fiber composites were used in adaptation.

The ASTM D638-10, devoted to tensile testing of polymers, was used to evaluate desired tensile properties. The I-type specimen ("dog bone") was employed in the tests, with dimensions $165\ mm \times 19\ mm$ (outer length and width, respectively) and thickness $3.3\ mm$, as depicted in Fig.2. The stacking sequences employed were either $[0°]_{11}$ or $[90°]_{11}$, oriented according to the tensile direction, to obtain properties respectively at the 1 or 2 direction illustrated in Fig.1.

The ASTM D3518-94, for determination of shear modulus and strength of laminated fiber composites, was used to evaluate shear properties of the 3D printed materials. Rectangular specimens as depicted in Fig.2 were used, with dimensions $25\ mm \times 200\ mm$ and thickness $4.8\ mm$. The stacking sequence employed was $[45°/-45°]_{4s}$ (symmetric), oriented according to the test direction.

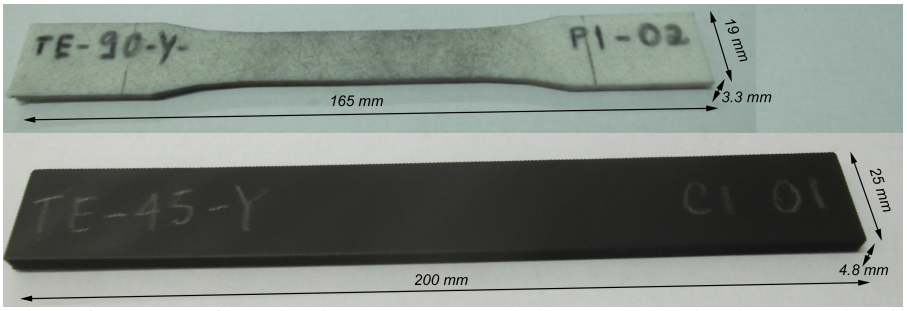

Figure 2: Employed specimens: tensile ("dog bone", upper) and shear (rectangular, lower). They illustrate the tested materials: the white is the PLA and the black is the PLA+CF.

For the production of all the tensile and shear specimens, the 3D printer was set to use only rectilinear infill with a volume fraction of 100%, which renders specimens without voids (as illustrated in Fig.1), whose material is deposited only in the predefined orientations defined by the aforementioned stacking sequences.

The 3D printer used for specimens manufacturing was an open source Prusa i3 Hephestos BQ, with a MK2a heatbed adapted and nozzle of 0.4 mm. In terms of printing parameters, the specimens were produced with printing (extrusion) temperature of $190°C$, deposition layer height of $0.3\ mm$, deposition line width of $0.33\ mm$, printing speed of $3000\ mm/min$ and heatbed at $70°C$. The PLA material employed is a commercial filament with diameter $1.75\ mm$ from BQ, made with the 4043D resin from NatureWorks. The PLA+CF is also a commercial filament with diameter $1.75\ mm$, made with the same base resin and with the addition of chopped short carbon fibers in 15% in weight, by ProtoPasta.

The experiments were conducted in an Instron 5500R universal testing machine. The specimens were loaded at a displacement rate of $1\ mm/min$. Strains in the specimens were monitored with the aid of a video gauge equipment,

an iMetrum NR. After mechanical testing up to failure, some specimens had their fracture cross sections inspected by scanning electron microscopy (SEM), using an equipment Zeiss Leo 435 VPi.

3. RESULTS

Figures 3, 4 and 5 show stress per strain curves acquired in testing samples of PLA and PLA+CF, printed at $0°$, $90°$ and $\pm 45°$. Each sample had five specimens tested. The data of the $0°$ samples were post-processed to obtain the E_1 tensile elastic modulus, the ν_{12} Poisson ratio and the S_1^* tensile strength. The data of the $90°$ samples were post-processed to obtain the E_2 tensile elastic modulus, the ν_{21} Poisson ratio and the S_2^* tensile strength. The data of the $\pm 45°$ samples were post-processed to obtain the G_{12} shear elastic modulus and the S_{12}^* shear strength. The results obtained for these properties of the PLA and PLA+CF are shown in Tables 1, 2 and 3.

From Tab.1, it is possible to notice that the addition of chopped carbon fibers in the PLA+CF increased the E_1 modulus about 2.23 times in comparison to the base PLA. Respectively, the E_2 modulus was raised about 1.25 times and the G_{12} modulus was raised about 1.16 times.

From Tab.2, it is possible to notice that the addition of chopped carbon fibers changed the Poisson coefficients of the base polymer. The ν_{12}, ν_{21} found for the PLA were more or less equal, around 0.3, but became respectively equal to 0.4 and 0.15 in the PLA+CF, a result close to that commonly found in unidirectional fiber reinforced materials, since the direction of the reinforcing fibers is stiffer.

The differences encountered in these properties of PLA and PLA+CF can be explained with the aid of the SEM images in Fig.6, 7 and 8, which show micrographs of fracture cross sections of PLA+CF specimens, respectively printed at $0°$, $90°$ and $\pm 45°$. In these images, details of the FDM process are noticeable, and it is possible to see the periodic microstructure of the printed specimens, which is a result of the deposition of equal fused material lines. Moreover, the chopped carbon fibers are the grayish cylinder-like structures dispersed in the PLA matrix. It can be seen that such fibers remained mostly aligned with the FDM printing direction in the PLA+CF, throughout the SEM images. This fact causes the biggest increase in stiffness in the direction of printing because this is the same direction in which the short fibers are mostly deposited, and therefore E_1 resulted bigger than E_2 in PLA+CF.This also explains why the PLA+CF material properties had a behavior similar to unidirectional fiber reinforced composites with respect to elastic coefficients.

From Tab.3, it is possible to notice that the addition of chopped carbon fibers did not alter consistently the strengths of the PLA and PLA+CF. This can be explained by the poor adhesion between the PLA and PLA+CF, already reported in the literature (Li *et al.*, 2016; Tian *et al.*, 2017).

Table 1: PLA and PLA+CF tensile and shear elastic moduli.

Property	Direction	PLA			PLA+CF			ASTM
		Max.	Avg.	Dev.	Max.	Avg.	Dev.	Standard
Tensile Modulus [MPa]	$0°$ (E_1)	3596	3376	212	7665	7541	96	D638
	$90°$ (E_2)	3340	3125	148	4145	3920	167	
In-plane Shear Modulus [MPa]	$\pm 45°$ (G_{12})	1140	1092	36	1270	1268	5	D3518

Table 2: PLA and PLA+CF Poisson coefficients.

Property	Direction	PLA			PLA+CF			ASTM
		Max.	Avg.	Dev.	Max.	Avg.	Dev.	Standard
Poisson Coefficient	ν_{12}	0.349	0.331	0.011	0.408	0.400	0.012	D638
	ν_{21}	0.336	0.325	0.014	0.163	0.150	0.008	

Table 3: PLA and PLA+CF material strengths.

Property	Direction	PLA			PLA+CF			ASTM
		Max.	Avg.	Dev.	Max.	Avg.	Dev.	Standard
Tensile Strength [MPa]	$0°$ (S_1^*)	56.1	54.7	1.9	53.7	53.4	0.2	D638
	$90°$ (S_2^*)	42.9	37.1	3.5	37.0	35.4	1.5	
In-plane Shear Strength [MPa]	$\pm 45°$ (S_{12}^*)	18.3	18.0	0.8	19.6	18.9	0.8	D3518

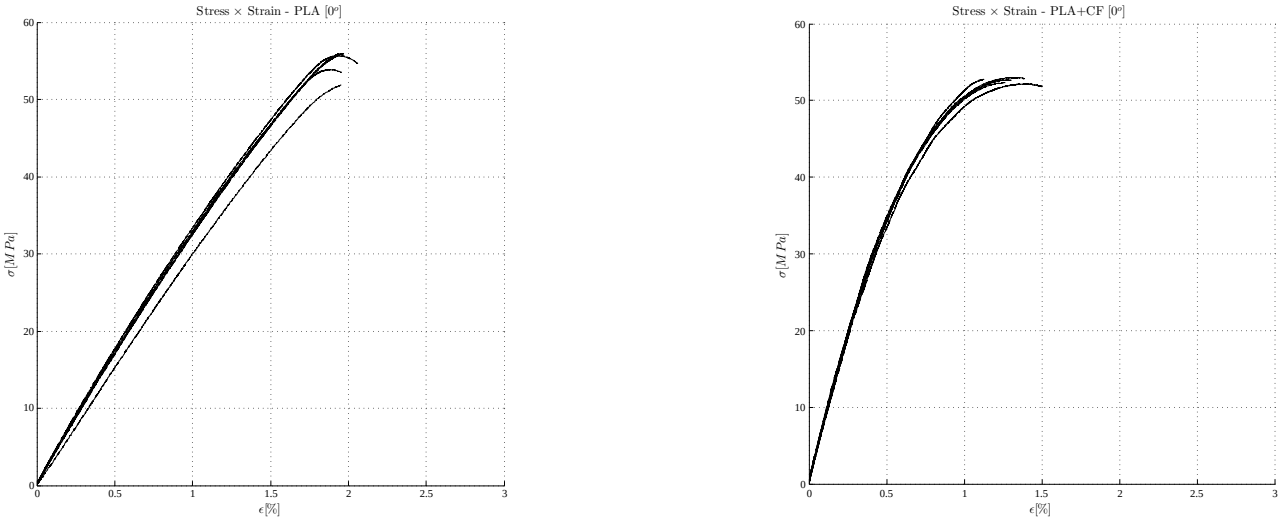

Figure 3: Stress $\times$ strain data for PLA and PLA+CF printed at $0°$.

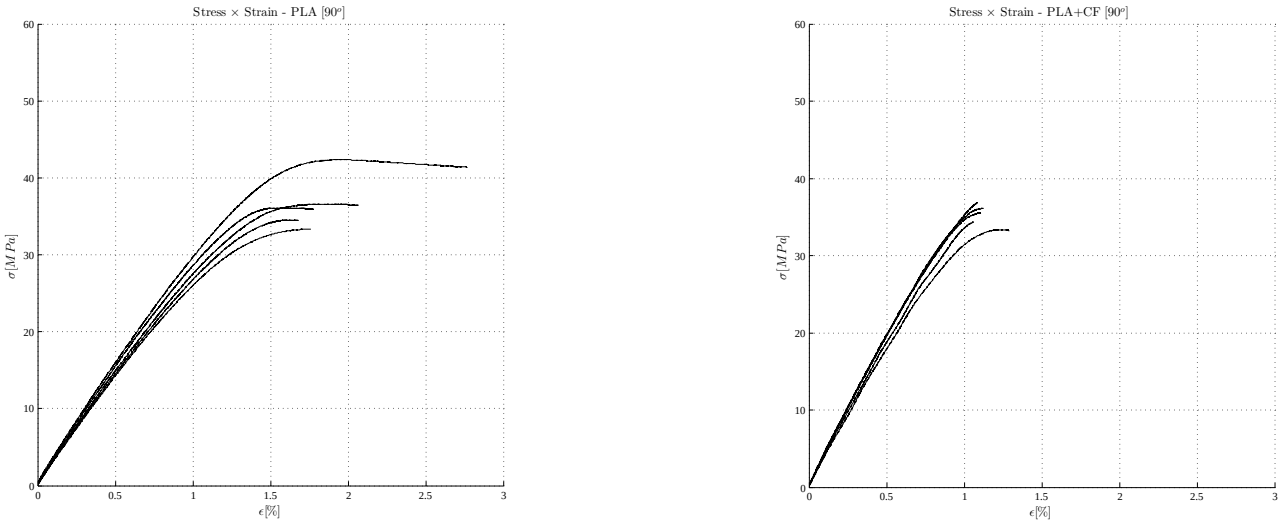

Figure 4: Stress $\times$ strain data for PLA and PLA+CF printed at $90°$.

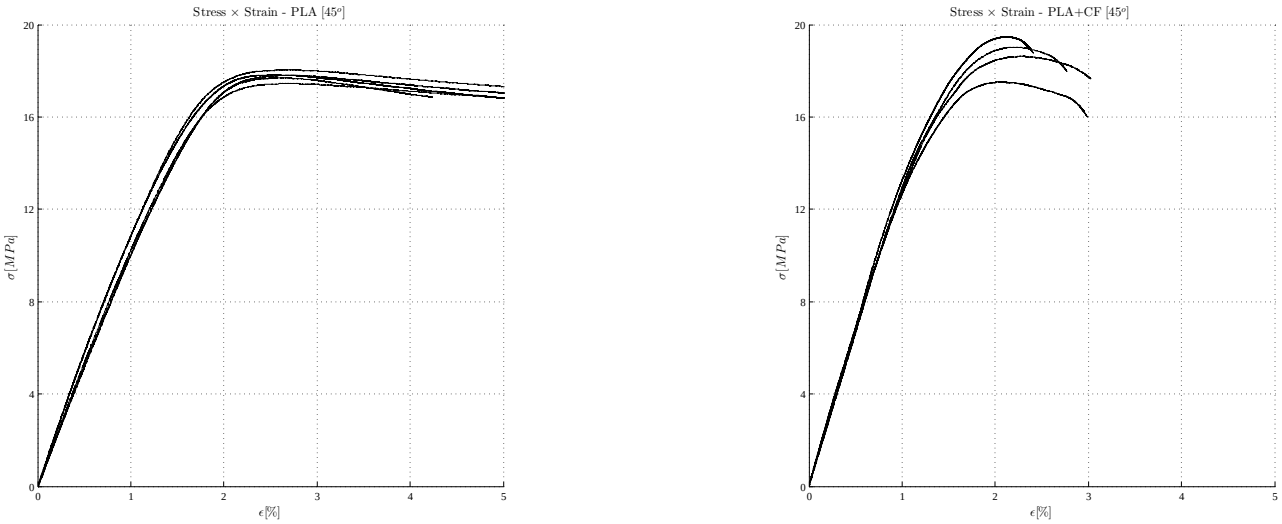

Figure 5: Stress $\times$ strain data for PLA and PLA+CF printed at $\pm 45°$.

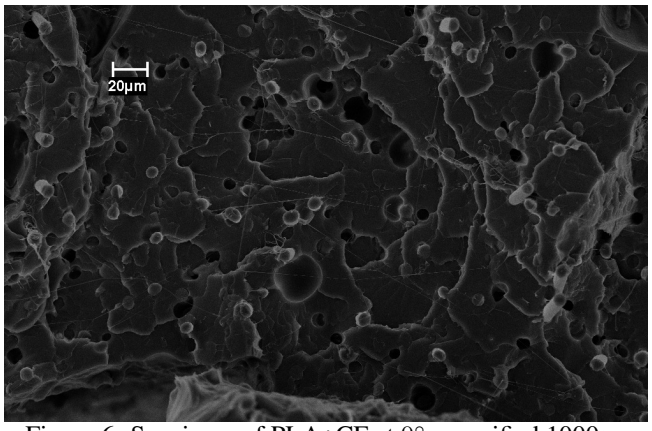

Figure 6: Specimen of PLA+CF at $0°$ magnified $1000\times$.

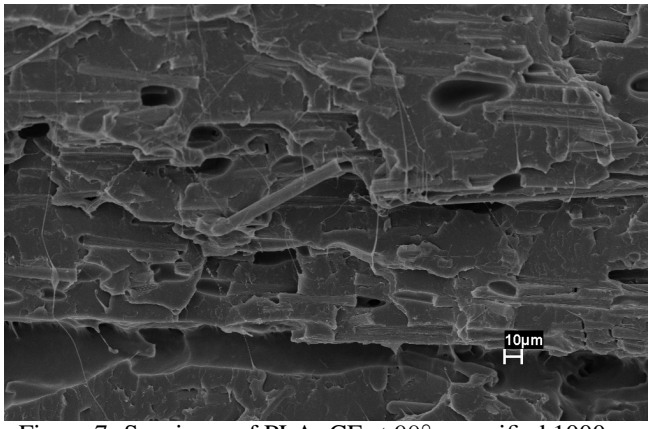

Figure 7: Specimen of PLA+CF at $90°$ magnified $1000\times$.

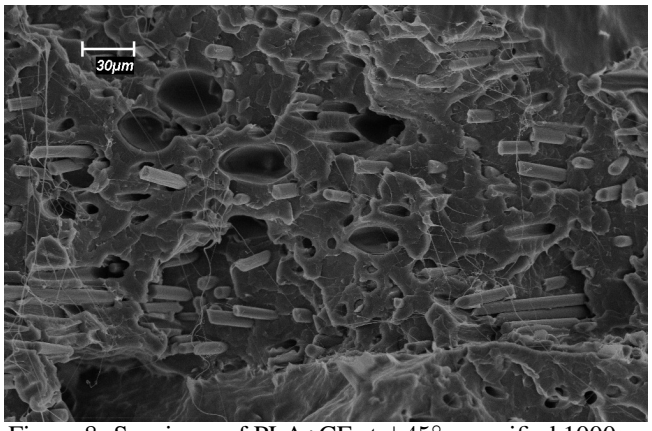

Figure 8: Specimen of PLA+CF at $\pm 45°$ magnified $1000\times$.

4. CONCLUSIONS

In this study, properties of a single PLA and a PLA+CF composite (a PLA reinforced with short carbon fibers of length about $60\ \mu m$, in a weight fraction of 15%) were measured for 3D printed specimens. The results obtained show that PLA+CF had its tensile stiffness in the direction of printing, E_1, consistently raised (about 2.23 times) in comparison to this same quantity on single PLA. Other measured stiffnesses like E_2 and G_{12} were also raised in PLA+CF but not as much as E_1. This increase in E_1 also resulted in changes in the measured Poisson ratios ν_{12}, ν_{21} for PLA+CF, which assumed average values of 0.4 and 0.15. In the other hand, the measured strengths S_1^*, S_2^* and S_{12}^* were not improved in the PLA+CF, in comparison with the PLA.

The results obtained for stiffnesses can be explained by the SEM micrographs seen in Fig.6 to 8. In these images, taken from the fracture cross sections of PLA+CF specimens, it is possible to see that the short carbon fibers (grayish cylinder-like structures) remained aligned with the 3D printing direction after the production of specimens by the FDM process. Therefore, it can be concluded that the most reinforced direction is the material deposition one in 3D printing, which explains the gains found for E_1, not found for other stiffnesses. With respect to strengths, they were not improved with the addition of short carbon fibers in the PLA+CF. However, the adhesion between PLA and carbon fibers is poor (Li *et al.*, 2016; Tian *et al.*, 2017), which results that such fibers were not able to improve the load carrying capability of the PLA at failure.

ACKNOWLEDGMENTS This work was supported by grants from ITA T-61 and FAPESP Process 2015/00159-5.

5. REFERENCES

ASTM. American Society for Testing and Materials, Standard test method for tensile properties of plastics. ASTM D638-10, 2010.

ASTM. American Society for Testing and Materials, Standard practice for reporting data for test specimens prepared by additive manufacturing. ASTM F2971-13, 2013.

ASTM. American Society for Testing and Materials, Standard test method for in-plane shear response of polymer matrix composite materials by tensile test of a +-45 laminate. ASTM D3518-13, 2013.

C. K. Chua and K. F. Leong. *3D printing and additive manufacturing: principles and applications*. World Scientific Publishing Company, Singapore, 5th. edition, 2017.

N. Li, Y. Li, and S. Liu. Rapid prototyping of continuous carbon fiber reinforced polylactic acid composites by 3D printing. *Journal of Materials Processing Technology*, 238:218–225, 2016.

F. Ning, W. Cong, J. Qiu, J. Wei, and S. Wang. Additive manufacturing of carbon fiber reinforced thermoplastic composites using fused deposition modeling. *Composites Part B*, 80:369–378, 2015.

J. N. Reddy. *Mechanics of laminated composite plates: theory and analysis*. CRC Press, Boca Raton, 1997.

X. Tian, T. Liu, Q. Wang, A. Dilmurat, D. Li, and G. Ziegmann. Recycling and remanufacturing of 3D printed continuous carbon fiber reinforced PLA composites. *Journal of Cleaner Production*, 142:1609–1618, 2017.

S. Upcraft and R. Fletcher. The rapid prototyping technologies. *Assembly Automation*, 23(4):318–330, 2003.

X. Wang, M. Jiang, Z. Zhou, J. Gou, and D. Hui. 3D printing of polymer matrix composites: a review and prospective. *Composites Part B*, 110:442–458, 2017.

6. RESPONSIBILITY NOTICE

The authors are the only responsible for the printed material included in this paper.